Chemical considerations for colloidal nanocrystal synthesis

Jonathan De Roo*

Department of Chemistry, University of Basel, 4058 Basel, Switzerland

E-mail: Jonathan.DeRoo@unibas.ch

Abstract

We take here the perspective of a nanochemist on the field of colloidal nanocrystals, focusing specifically on nanocrystal synthesis. Considering the three components of a colloidal synthesis, we discuss the chemistry that occurs with precursors, ligands, and solvents. Insight into the coordination chemistry and the organic chemistry of nanocrystal syntheses brings us one step closer to a retro–synthetic analysis of a nanocrystal reaction. We also reflect on different crystallization mechanisms (either under thermodynamic or kinetic control). We consider the possibility that the different models are simply describing different experimental conditions and are not fundamentally at odds with one another. However, we do critically evaluate the use of the terms *monomer* and *burst nucleation*. Finally, we discuss good chemical practices for a nanochemist, and we try to define nanocrystal purity. This perspective will hopefully inspire researchers in colloidal nanoscience to think more about chemical equations, consider reaction by–products, and come together as a field to agree on standard reporting practices for colloidal nanocrystals.

1 Introduction

The modern field of colloidal nanocrystals started in 1993 with the seminal paper of Murray, Norris and Bawendi.[1] The formation of CdSe, CdS and CdTe nanocrystals was reported from dimethylcadmium, tri-*n*-octylphosphine (TOP), tri-*n*-octylphosphine oxide (TOPO) and an appropriate chalcogen precursor. This report contained the basic components for the following three decades of research; precursors that convert at high temperature in the presence of surfactants (ligands), thus forming colloidal objects that are organic/inorganic hybrids. While gold colloids could already be synthesized since 1951 — Turkevich, Stevenson and Hillier reported that gold salts are reduced by citrate in boiling water to gold nanocrystals[2] — the use of surfactants, nonpolar solvents and high temperature provided much finer size control, and allowed access to materials with higher crystallization temperatures or with higher complexity.

Over the years, the field has acquired more control over the nanocrystal size distribution,[3] shape,[4] composition,[5] and heterostructure,[6] while at the same time using safer, less toxic precursors.[7] A historic overview of the development of semiconductor nanocrystals (called quantum dots) was recently provided by Efros and Brus, who stood at the genesis of their field.[8] Although CdSe was long the prototypical nanocrystal, many different types of nanocrystals have been produced,[9] e.g., III-V semiconductors,[10] plasmonic oxides,[11] refractive oxides,[12,13] metals,[14–16] and metal halides.[17,18] Once their size distribution was minimized such that the ensemble could be deemed *monodisperse*, nanocrystals have been developed as meta-atoms; nanometer-sized building blocks for microscale and macroscale matter.[19,20] Nowadays, nanocrystals are optimized as heterogeneous catalysts,,[21,22] as battery electrodes,[23] as downconverters in LEDs,[24,25] etc.

While nanocrystals have exciting applications, it is useful to reflect on the chemistry that is responsible for their formation. Has the field reached a level of maturity that enables retro–synthesis of colloidal nanocrystals? Can we write a balanced chemical mechanism for precursor conversion and/or crystallization? Are we considering the nature of possible by–

products in our purification strategies? These are only some of the questions that we try to answer in this perspective.

While synthesizing nanocrystals is sometimes referred to as *cooking* nanocrystals, it is the goal of the nanochemist to elevate this intuitive skill into reproducible science. A colloidal synthesis has three essential components: precursors, surfactants and solvent. We will first discuss the chemistry associated with each of these three components (which involves coordination chemistry and organic chemistry). Subsequently, we ask ourselves the question as to how nanocrystals crystallize, i.e., how they nucleate and grow. There are two mainstream models for nucleation and growth, which either function under thermodynamic control or kinetic control. Finally, we reflect on good chemical practices for the nanochemist and discuss reagent purity and product purity. Conceptualizing a colloidal synthesis as a sequence of (many) chemical reactions, we can draw parallels to typical organic chemistry endeavours such as the total synthesis of a natural product. In contrast to organic total synthesis, colloidal nanoscience does not yet have a history of applying a retro–synthetic analysis. It is the ambition of many nanochemists to achieve a level of mechanistic understanding that enables the retro–synthesis of particular nanocrystal shapes, compositions, sizes and heterostructures.[6,26]

2 The chemistry of precursor conversion

Precursors are molecules or metal complexes that contain the individual elements of the final nanocrystal in a different form. Therefore, the first step in colloidal synthesis is usually the conversion of the precursors into the intended product. Given its importance, precursor conversion has been studied in many nanocrystal systems: metals,[14,27–30] metal sulfides and selenides,[7,31–35] metal oxides,[36–38] lead halides,[39] and metal pnictides.[40–43] In such efforts, nanochemists aim to write down the complete and balanced chemical equation, after determining the correct stoichiometry of the reaction and identifying reaction by–products.

Ideally, this is complemented with a rigorous kinetics study to obtain further details about the mechanism. Mechanistic insight is very useful to develop new syntheses and to optimize existing ones. We will discuss here a few selected examples from our own research.

2.1 Disproportionation to InP

InP can be synthesized by reacting InX_3 salts (X = Cl, Br, I) with aminophosphines, *e.g.,* $P(NEt_2)_3$, in oleylamine solvent (which also acts as a surfactant and as a reagent).[44,45]

$$InX_3 + P(NEt_2)_3 \xrightarrow[oleylamine]{} InP \tag{1}$$

While indium is already is the correct oxidation state, phosphorus needs to be reduced. Oleylamine is often playing the role of reductant, but not in this case. Here, 75 % of the phosphorus is oxidized to reduce the other 25 % (i.e., a disproportionation reaction).[40,46] The disproportionation does not occur directly with the secondary aminophosphine precursor, but requires a primary aminophosphine. The diethylaminophosphine thus first undergoes a transamination reaction with oleylamine.

$$P(NEt_2)_3 + 3\,RNH_2 \longrightarrow P(NHR)_3 + 3\,HNEt_2\uparrow \tag{2}$$

Subsequently, three equivalents of oleylaminophosphine reduce a single P(+III) to P(-III), see Scheme 1. Three equivalents of tetra(oleylamino)phosphonium chloride are formed as by–products. The fully balanced chemical equation for this reaction becomes

$$InX_3 + 4\,P(NEt_2)_3 + 12\ RNH_2 \longrightarrow InP + 12\,HNEt_2\uparrow + 3\ [P(NHR)_4X] \tag{3}$$

This chemical equation rationalizes what appeared to be a strange experimental observation: the need for 4 equivalents of the aminophosphine to reach full yield in indium. By understanding this mechanism, nanochemists could also understand why a similar strategy

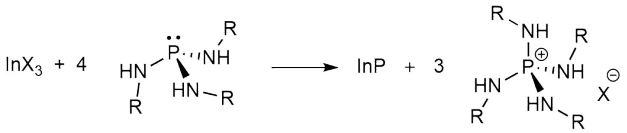

Scheme 1: Disproportionation reaction of aminophosphines, forming InP nanocrystals.[40]

for synthesizing InAs failed; the aminoarsine precursors ($As(NR_2)_3$) do not disproportionate. Fortunately, three equivalents of aminophosphine can reduce one equivalent of aminoarsine, and InAs quantum dots were successfully formed according to:

$$InX_3 + As(NEt_2)_3 + 3\,P(NEt_2)_3 + 12\ RNH_2 \longrightarrow InAs + 12\,HNEt_2\uparrow + 3\ [P(NHR)_4X] \quad (4)$$

2.2 Secondary aldimines as key intermediate in nitride formation

Copper nitride nanocrystals are typically synthesized by a simple heat-up method.[47–49] Copper nitrate is heated in oleylamine and after 15 min at 260 °C, copper nitride nano-cubes are formed with a cube edge length of around 10 nm.

$$Cu(NO_3)_2 \cdot 3\,H_2O \xrightarrow[oleylamine]{} Cu_3N \quad (5)$$

We found that Cu(II) is first reduced to Cu(I) by oleyamine around 190 °C.[43] The by–products are: a primary aldimine and two protons, see Scheme 2. We experimentally confirmed the 2:1 stoichiometry of copper to amine. This is an exciting result because it shows the complete and balanced redox reaction, including by-products that can be easily overlooked such as protons. We conclude that oleylamine is a two–electron reductant. Aldimine seems to be the general oxidation product of oleylamine as it has also been identified in the synthesis of Cu(0) and Pd(0) nanocrystals from metal acetylacetonate precursors.[50,51]

As a second part of our investigation, we focused on the source of nitride in copper nitride.[43] The nitrate anion also oxidizes primary amine to a primary aldimine, albeit at slightly higher temperatures (above 220 °C). The primary aldimine, produced by both

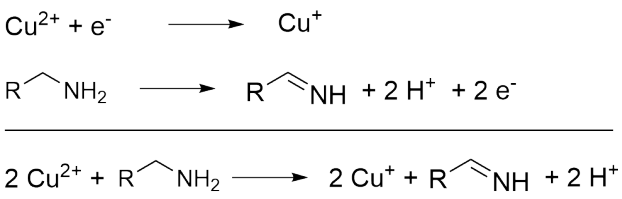

Scheme 2: Redox half reactions and overall redox reaction for the reduction of Cu^{2+} by primary amines.[43]

oxidation mechanisms, reacts further with another equivalent of oleylamine to a secondary aldimine, concomitantly eliminating ammonia. Ammonia reacts with Cu(I) to copper nitride (again releasing three protons). The overall pathway is shown in Scheme 3.[43] There is a high similarity with the pathway towards InN formation,[52] where In(III) is reduced to In(0), forming also the primary aldimine. The secondary aldimine formation and ammonia release thus seems a useful mechanism to produce nitrides, which are generally a challenging and underdeveloped nanomaterials class.[53]

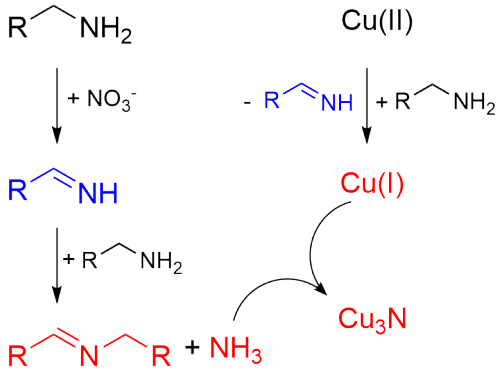

Scheme 3: The proposed pathway for Cu_3N formation. Precursors are shown in black, detected species in red, and hypothesized intermediates in blue.[43]

2.3 ZrO_2 formation by E1 elimination

Very high quality (*i.e.,* crystalline, colloidally stable and monodisperse) nanocrystals of zirconia can be synthesized from zirconium chloride and zirconium isopropoxide in tri-*n*-

octylphosphine oxide.[13]

$$1.25\ \mathrm{ZrCl_4} + \mathrm{Zr(O}i\mathrm{Pr)_4} \cdot i\mathrm{PrOH} \xrightarrow[TOPO]{0.45\,mol/kg,\,340^{\circ}\mathrm{C}} 2.25\ \mathrm{ZrO_2} + 5\ i\mathrm{PrCl} \tag{6}$$

While the above equation captures the zirconia formation, it is based on two assumptions: (1) the coordinated isopropanol participates in the reaction, and (2) the reaction proceeds through an S_N1 substitution mechanism, producing isopropyl chloride. We have recently shown that the reaction mixture contains mixed chloroalkoxide species: $\mathrm{ZrCl_3(O}i\mathrm{Pr)}$ and $\mathrm{ZrCl_2(O}i\mathrm{Pr)_2}$.[38] These species are unreactive towards isopropanol and thus only a stoichiometric amount of zirconium chloride is required in the reaction. We also provided evidence for an alternative mechanism based on E1 elimination, see Scheme 4. After ligand redistribution and condensation in $\mathrm{ZrO_2}$, we found that $\mathrm{ZrCl_4}$ is retrieved as a by–product of the reaction. Also the formation of isopropanol was confirmed. We estimated the relative contribution of the E1 and S_N1 mechanism as 80 : 20. Using this new mechanistic insight, we adapted the synthesis to optimize the yield and gain control over nanocrystal size. By repeatedly injecting zirconium isopropoxide in the reaction mixture, the $\mathrm{ZrCl_4}$ by–product is consumed and the reaction is extended. As a result, the nanocrystals grow to larger sizes and the yield increases significantly.[38]

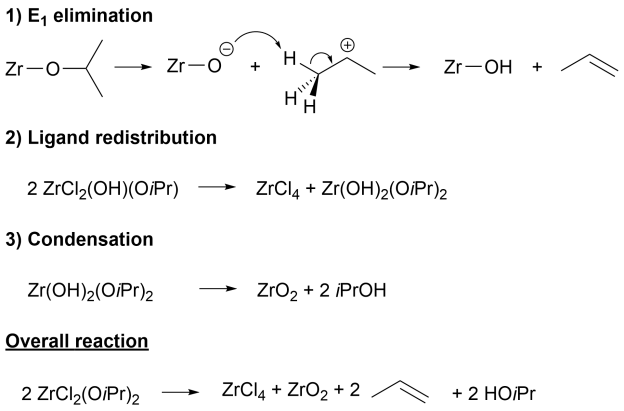

Scheme 4: Our alternative pathway for the formation of zirconia nanocrystals is based on E1 elimination, ligand redistribution, and condensation reactions. Reproduced from reference.[38] Copyright 2022 American Chemical Society.

The cases of zirconia and InP clearly show that mechanistic understanding directly enables the nanochemist to go further than the state-of-the-art. Either new materials could be formed or the size was tuned. However, we are only scratching the surface in terms of mechanistic insight. We indeed managed to write a balanced chemical equation, but the next step is a detailed analysis of the kinetics. We are currently pursuing this avenue for group 4 metal oxide nanocrystals.

3 The chemistry of ligands

Surfactants, or ligands in general, are an important component of colloidal synthesis. They have typically long aliphatic chains and a polar binding group. Ligands form complexes with metal precursors, providing solubility in the typically used nonpolar, high boiling solvents. In addition, ligands bind to the nanocrystal surface, providing colloidal stability. While a colloid has usually a colloidal stability (i.e., a metastable state), it was shown that very small nanocrystals have an equilibrium solubility.[54–56] To differentiate from the regular solubility of a solid, the term *colloidal solubility* was introduced.[57] For small nanoparticles, the colloidal solubility is not determined by core–core interactions, but rather by the crystallization behaviour of the ligands.[58,59] Branched chains, chains with double bonds, or mixtures of long and short chains, are all effective in preventing ligand crystallization on the nanocrystal surface, and thus provide a high colloidal solubility.[55,60]

Ligands have thus an important function, but they can also be involved in side–reactions. The ligand oleylamine is often involved in precursor conversion chemistry,[61] see also the previous section. In general, one cannot assume that the ligands added to the reaction, are also the ligands ending up on the final nanocrystal surface. Ligands are not per definition inert but ligand transformations have received a lot less attention than precursor conversion. We will discuss here a few examples were we found (sometimes surprising) ligand transformations, usually with important consequences for the final nanocrystal.

3.1 Decomposition of TOPO

During the synthesis of TiO_2, ZrO_2, and HfO_2 nanocrystals at 300–360 °C, the ligand/solvent tri-*n*-octylphosphine oxide (TOPO) oxidizes to dioctylphosphinic acid and octylphosphonic acid.[62] The octylphosphonic acid dehydrates and forms an anhydride. Although the oxidation only proceeds to a small extent (probably consuming adventitious oxygen), the formed decomposition products have a much higher affinity for the metal oxide nanocrystal surface than TOPO itself. Thus, the nanocrystal surface adsorbs the decomposition products and the surface becomes highly complex with three different species present, see Figure 1. 1–octene is a by–product of the oxidation, and is observed refluxing in the reaction setup.[63]

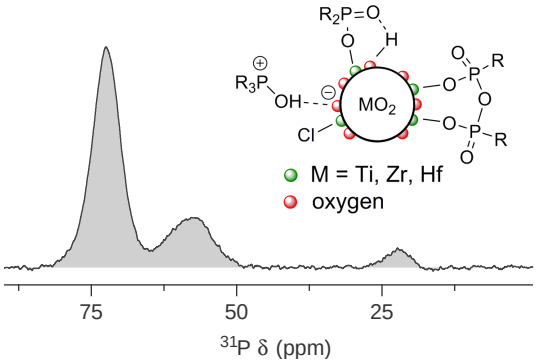

Figure 1: Titanium, zirconium and hafnium oxide nanocrystals synthesized in TOPO are capped with TOPO and its decomposition products, resulting in a complex ligand shell. The three species are present in the phosphorus NMR spectrum. Adapted from reference.[62] Copyright 2017 American Chemical Society.

3.2 Oxidation of oleylamine to oleic acid

We established in the previous section that oleylamine is oxidized to aldimine by nitrate. We recently found that the reaction does not stop there but can proceed all the way to carboxylic acid.[64] As a model system, we investigated the synthesis of CeO_2 nanocrystals, from cerium nitrate and oleylamine.

$$Ce(NO_3)_3 \cdot 6\,H_2O + RNH_2 \xrightarrow[hexadecane]{} CeO_{2-x} \tag{7}$$

The metal nitrate forms first a complex with oleylamine, which subsequently decomposes, producing a myriad of by–products, see Scheme 5 . The primary aldimine is hydrolyzed by adventitious water to aldehyde, which is further oxidized to carboxylic acid (presumably by nitrate or one of the nitrous decomposition products). Since carboxylates has a higher binding affinity to oxide surfaces that oleylamine, the final particles were capped with carboxylate and not with oleylamine.[64] Interestingly, nickel, zinc and zirconium nitrate show a similar reactivity. Also in the case of copper nitrate, carboxylate is retrieved at the copper nitride nanocrystal surface, albeit as a co-ligand with oleylamine.[43]

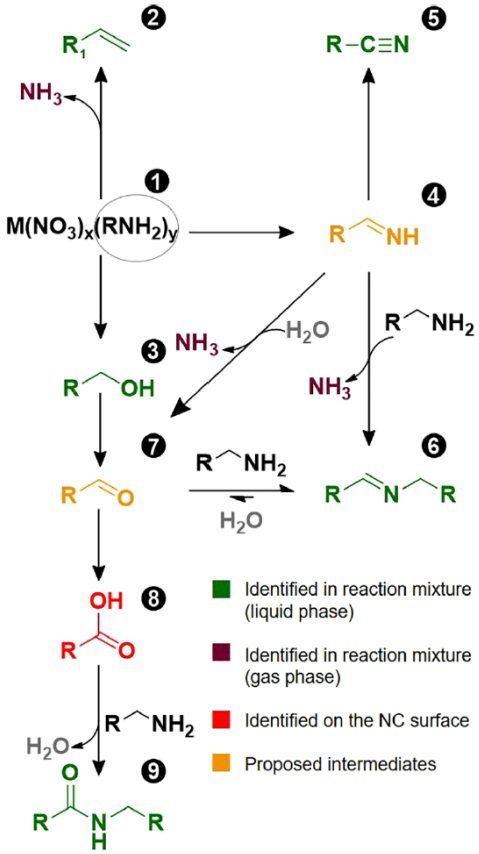

Scheme 5: Proposed Reaction Path for the Formation of Carboxylic Acid through the Oxidation of Coordinated Alkylamines by Nitrate. Reproduced from reference.[64] Copyright 2021 American Chemical Society

3.3 Oligomerization of phosphonic acid

Phosphonic acids are often used for colloidal syntheses above 300 °C since metal carboxylates decompose at these temperatures.[65,66] Phosphonic acids do not decompose but still dehydrate to form phosphonic acid anhydride, see Scheme 6.[31,67] The reaction can proceed with the second acidic group, producing phosphonic acid anhydride oligomers. In the presence of this oligomer, CdSe nanocrystals can aggregate or form a gel.[68]

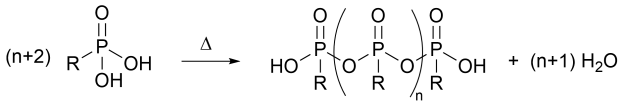

Scheme 6: Formal dehydration of phosphonic acids. In practice, often a dehydration agent is also present in the reaction mixture. Reproduced from reference.[67] Copyright 2022 American Chemical Society

To prevent gelation, we developed a new ligand class: mono–alkyl phosphinic acids.[67] When substituting phosphonic acids with mono–alkyl phosphinic acids, no mascroscopic gels were formed, and the ease of nanocrystal purification improved significantly. Interestingly, the reactivity of the cadmium phosphinate was intermediate to the reactivity of cadmium phosphonate and cadmium carboxylate. This provides the nanochemist with an additional handle on the reaction kinetics, which is currently mostly controlled by the chalcogen precursor.[33,34,69]

The chemistry of ligands is usually undesired or at least surprising. While we were able to discern certain chemical pathways, a fully balanced chemical equation is often missing since elusive gaseous reagents or by–products are involved. Since ligands modulate the nucleation and growth of nanocrystals (see further), the changing ligand composition in the reaction mixture is likely to have an important effect. The kinetics of these ligand transformations are thus highly relevant, yet unknown.

4 The undesired chemistry of solvents

A crucial element of a colloidal synthesis is the solvent, which is ideally an innocent bystander. Some ligands such as oleylamine and TOPO are also often used as solvent, but other solvents are only meant as a heat transfer medium. However, nanocrystal syntheses require high temperatures and often aggressive reagents. Few chemicals are able to remain truly inert under such conditions. For example, 1-octadecene (ODE) is a popular (and economical) solvent. Unfortunately, ODE polymerizes at temperature above 120 °C and produces significant amounts of polymer over the course of a nanocrystal reaction at 240–320 °C.[70] Given the similar size and polarity of ligand–capped nanocrystals and poly(ODE), purification is very difficult using precipitation/redispersion cycles or size exclusion chromatography (SEC).[70] Poly(ODE) is therefore most likely the cause for many (unpublished) anecdotes on gels and oils that researchers obtain during the purification process. Polymerized ODE can also be responsible for a visual turbidity, for example in the case of TiO_2 platelets synthesized according to Gordon et al, see Figure 2.[71] One of the reagents (TiF_4), acts as a polymerization catalyst, exacerbating the problem. For many reactions, ODE can be easily replaced by hexadecane (liquid at room temperature, bp = 287 °C) or octadecane (solid at room temperature, bp = 320 °C), resulting in particle ensembles that are much easier to purify.

Other solvents such as TOPO and oleylamine have been investigated but since they are also ligands, they were discussed in the previous section. While squalane is likely to be inert, squalene has multiple double bonds. Given that the double bonds in squalene are highly substituted they are much less reactive, but under the right conditions, even squalene could exhibit side–reactions. Diphenylether is another solvent that should be investigated.

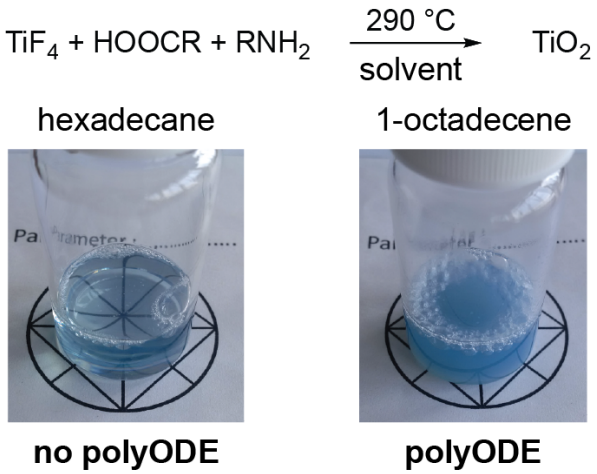

Figure 2: During the formation of titania nanoplatelets in ODE, also a large amount of polymerized ODE is formed, which is macroscopically visible as turbidity. Using hexadecane as solvent, the dispersion is clear and transparant.[70]

5 Crystallization into nanocrystals

After (or during) precursor conversion, the constituting atoms have to come together in an organized fashion (crystallization), preferably forming highly monodisperse nanocrystals with control over size, shape, composition, crystal structure and heterostructure. From a chemical perspective, it is extremely impressive that a one–pot synthesis with thousands of simultaneous reactions produces these rather uniform objects containing several thousands of atoms. Perfect atomic precision can be obtained for very small clusters but is generally elusive for larger sizes.[72]

When addressing crystallization, a distinction is usually made between the formation of new particles (nucleation) and the growth of existing particles. For a finite amount of precursor, the balance between nucleation and growth determines the final number of particles and thus the particle size (at full yield). Indeed, more nucleation increases the number of particles. Since the same amount of material is distributed over more particles, the final particle size will be smaller. In the literature, there are several theories and approaches that aim to describe the process of nucleation and growth. They can be roughly divided in thermodynamic models (basel on classical nucleation theory) and kinetic models. We will discuss

their assumptions, conclusions, advantages and disadvantages in the follow paragraphs. Interestingly, some key insights were provided by both models. It is therefore good to keep in mind that a model is just that; a model. Not necessarily reality, models help us conceptualize and to predict reaction outcomes. The nanochemist should be open to (radically) changing the model when confronted with convincing (dis)proof.[73]

5.1 Thermodynamic models of nucleation and growth

In the following, we will assume that the nanocrystal synthesis proceeds via a relatively slow precursor conversion step.[69,74,75]

$$\mathrm{P} \xrightarrow{slow} \mathrm{M} \overset{fast}{\rightleftharpoons} \mathrm{NC} \tag{8}$$

The conversion of precursor (P) generates a monomer (M). The monomer is defined as a soluble building block. In the case of sulfur droplets, the monomer could be the S_8 molecule. In the case of ice crystals, the monomer is a water molecule. In the case of hexane droplets in the gas phase, the monomer is a hexane molecule. In the case of gold nanocrystals, the monomer can be conceptualized as a single Au(0) atom dissolved in water. Equation 8 further assumes that crystallization (nucleation and growth) into a nanocrystal (NC) is fast compared to precursor conversion.

Classical nucleation theory (CNT) describes the thermodynamics of particle formation. CNT considers that every particle is in equilibrium with its constituting monomers, dissolved in solution.

$$\mathrm{n\,M_{(l)}} \rightleftharpoons (\mathrm{M})_{\mathrm{n}} \tag{9}$$

Assuming a spherical particle, the change in free energy associated with Equation 9 is written as:

$$\Delta G(n) = -nk_BT \ln S + \gamma a_m n^{2/3} \tag{10}$$

where we defined the supersaturation ratio

$$S = \frac{[M]}{[M]_{eq}}$$

and

$$a_m = 4\pi \left(\frac{3v_m}{4\pi} \right)^{2/3}$$

v_m is the volume of one monomer and γ is the surface tension. The formation of a particle is thus driven by a favorable bulk term ($-nk_BT \ln S$) but inhibited by an unfavorable surface term ($\gamma a_m n^{2/3}$). For small particles the surface term is dominant ($\Delta G(n) > 0$) while for larger particle the bulk term compensates for the surface energy ($\Delta G(n) < 0$), see Figure 3A. This leads to the phenomenon of a *critical radius*, from which growth (attachment of one monomer) becomes favorable. The ΔG necessary to form a particle with the critical radius is the activation energy for nucleation, and it strongly depends on the supersaturation.[3,76,77]

In a seminal paper in 1950, LaMer and Dinegar studied the growth of sulfur colloids in water.[79] They postulated that nucleation happens infinitely fast (in a burst) once the supersaturation reaches a critical point, see Figure 3B. All particles are formed during this short period of time and subsequently grow uniformly by diffusion limited growth. This was a first attempt to rationalize how colloidal syntheses can produce monodisperse particles. It is important to recognize that *burst nucleation* was an assumption of LaMer and Dinegar and not an observation. Nevertheless, the three phases of the LaMer model (monomer build up, burst nucleation, diffusion limited growth), and the requirement of separating the nucleation step from the growth step to produce monodisperse particles, have been widely accepted as a fact, until recently.[26,80,81]

At any time during a nanocrystal synthesis, the change in monomer concentration is determined by:

$$\frac{d[M]}{dt} = Q - n^* J_N - G\, n_p \tag{11}$$

Q is the precursor–to–monomer conversion rate, J_N is the nucleation rate (n^* is the amount

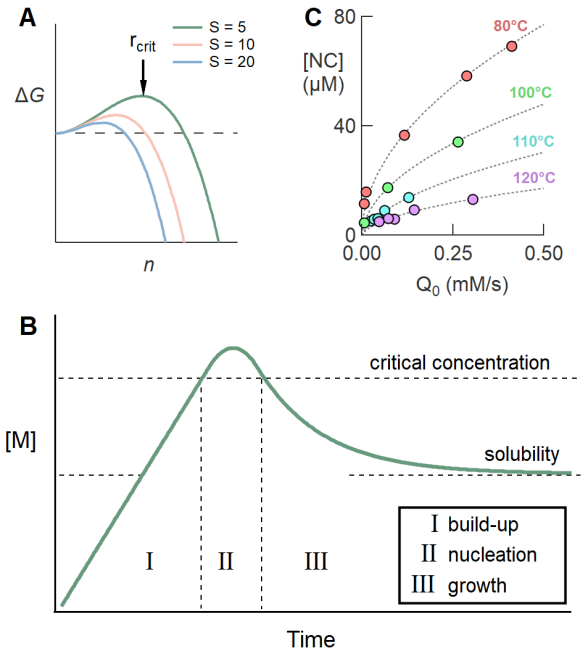

Figure 3: (A) Change in free energy upon the formation of a particle from n monomers (B) Diagram of the LaMer model, featuring monomer build-up, burst nucleation and diffusion limited growth. (C) Relation between final number of particles and monomer generation rate, exemplified here with the concentration of PbS nanocrystals at different temperatures. Data replotted from reference.[78]

of monomer in a nucleus) and G is the growth rate (n_p is the number of particles). Sugimoto and others solved this mass balance under the assumption of burst nucleation and found that the particle number is proportional to Q and inversely proportional to the growth rate.[82–84]

$$n_p \sim \frac{Q}{G} \tag{12}$$

The above linear dependence on Q is valid for high growth rates.[82,83] For lower growth rates (e.g., in the presence of surfactants) a square root dependence is predicted.[84] Such relations between precursor conversion rate and particle number have been confirmed by ample experimental data,[33,34,69,74,78,83,85,86] see Figure 3C for an example of PbS nanocrystals.

Numerical simulations have also come to the same conclusion.[74] For simulations, exact expressions for the nucleation and growth rate are needed. Using the activation energy for nucleation, an Arrhenius type expression for the nucleation rate was implemented.[74,75] One can also derive a generalized growth rate, based on thermodynamic considerations and Fick's law of diffusion.[87] In case the diffusion of the monomer towards the surface is slower than the incorporation rate, the system is under diffusion control. When the incorporation rate is much slower than the diffusion rate, the system is in reaction control. Under reaction control, larger particles grow faster than smaller particles. This leads to a broadening of the size distribution and is called *size defocusing*. Under diffusion control, there is a region where small particles grow faster than large particles and this *size focusing* effect was an important argument of LaMer and Dinegar, to explain the formation of monodisperse colloids.

The advancement of analytical methods has provided the scientific community with the necessary tools to investigated nucleation in greater detail than was possible in 1950.[88] Small angle X-ray scattering (SAXS), for example, has been instrumental in disproving the concept of burst nucleation.[89,90] In the case of Pd, CdSe, InP and PbS(e) nanocrystals, researchers clearly observe a steady increase of the particle number throughout a large portion of the reaction time,[78,89–91] see Figure 4 for an example on Pd nanocrystals. Therefore, the reaction

displays *continuous nucleation* rather than burst nucleation. The ability to nonetheless form monodisperse ensembles is explained by a strongly size–dependent growth rate, since the modest size focusing provided by diffusion–limited growth is unable to account for the extreme size focusing (superfocusing) that must be occurring. A simple reaction–limited growth expression was proposed.[90]

$$G = \frac{k}{r^n} 4\pi r^2 [M] \tag{13}$$

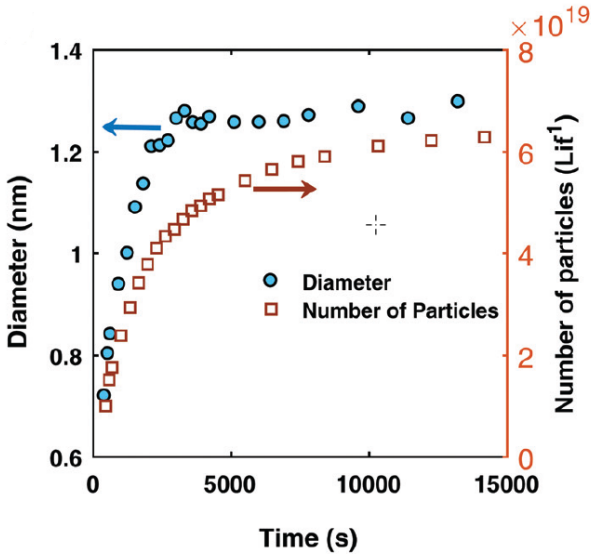

Figure 4: The number of palladium particles keeps increasing over the course of the reaction, suggesting continuous instead of burst nucleation. Reproduced from reference[89] with permission from the Royal Society of Chemistry

One recognizes in this equation the functional form of a regular chemical kinetics equation. For $n > 2$, the growth rate is strongly size focusing. The hypothesis is thus that small particles have a higher intrinsic growth rate, while big particles are deactivated for growth.[90] The origin of this phenomenon is not yet perfectly clear. It could be due to decreasing particle curvature, which forces the ligand chains closer together, leaving less space for the monomer to penetrate the ligand shell. Or it could be that ligands are more tightly bound to larger nanocrystals with mature facets. It is interesting that in case of InP, PbS and PbSe, the

maximum attainable nanocrystal size increases with the reaction temperature.[78,91] At higher temperatures, the activation barriers for growth are thus more easily overcome or perhaps the ligands are involved in a temperature dependent adsorption–desorption equilibrium. Finally, superfocusing does not only explain the narrow size distribution despite of continuous nucleation, it is likely directly *responsible for* continuous nucleation.[90] Consider the following thought experiment. There is a steady monomer generation. Once the critical supersaturation is reached, nuclei are formed. Upon growth, the growth rate rapidly decreases while the monomer generation continues. As a result, the monomer concentration builds up again, the critical supersaturation is reached and a new nucleation event takes place. One thus sees that continuous nucleation is not at odds with the ideas of classical nucleation theory. Continuous nucleation is simply a consequence of a size–dependent growth rate. The burst nucleation concept of LaMer on the other hand, is no longer a valid model in the face of current evidence.[78,81,89–91] It seems puzzling that the predictions of Sugimoto and others (based on burst nucleation) are correctly describing the relation between precursor conversion rate and particle number. It would thus be interesting to analyze with simulations how continuous nucleation fits in this picture.

5.2 From thermodynamic to kinetic control

Although we have not yet dismissed classical nucleation theory, we should analyse its assumptions again. First, CNT relies on the concept of a monomer. While the monomer was introduced above in an intuitive way, the examples were chosen such that there could be no confusion. For materials like CdSe or ZrO_2, the concept of a monomer is less straightforward. Does precursor conversion really deliver a CdSe or ZrO_2 unit? Any chemist would be hard–pressed to write a reasonable Lewis structure for such "monomers". In the case of zirconia, one could argue that $Zr(OH)_4$ makes more sense as a monomer. However, condensation of the hydroxide into oxo bridges happens concurrently with the precursor conversion into the hydroxide and thus $Zr(OH)_4$ is an elusive species. In the case of PbS and PbSe,

we recently analyzed the induction delay time between precursor injection and crystal formation.[78] Presumably this induction delay is the first phase of the LaMer diagram with monomer build–up. Using X–ray total scattering and Pair Distribution Function analysis, we found indeed evidence for a solute, a soluble dimer capped with two additional lead oleate Z–type ligands; $Pb_2(\mu_2{-}S)_2(Pb(O_2CR)_2)_2$.[78] In the case of iron oxide nanocrystals, the iron oleate *precursor* was shown to be already a trimeric oxo cluster with an Fe_3O core, capped by oleate ligand.[81] Such studies are rare but absolutely necessary to build up a molecular picture of both precursor conversion and crystallization.

A second limitation of CNT is the requirement for reversibility. CNT appears suitable to describe the formation of alkane droplets in the gas phase. These droplets are held together by weak London dispersion forces between the monomers (the alkane molecules) and thus the whole system is reversible and in thermodynamic control. Finke et al. recently argued that CNT is not applicable to systems with stronger bonds between the "monomers", such as Ir nanocrystals.[80,92] Strong metallic bonding or covalent bonds are not easily broken and the requirement for chemical reversibility is not satisfied. The reaction is thus under kinetic control. This might be also reflected in the difficulty in obtaining highly crystalline InP and GaP nanocrystals (materials with a high covalent character).[93] A word of caution regarding crystallization and reversibility is in order. Crystallization requires a certain reversibility in bond forming and bond breaking for the structure to adopt the ordered, minimum energy configuration. Taking the example of cubic zirconium oxide (where zirconium has a coordination number of eight), this means that the material needs to break a few bonds (not all eight) to rearrange the structure. It does not mean that a ZrO_2 monomer needs to dissolve completely. Even systems where the monomer does not redissolve (defined here as kinetic control) could thus still lead to crystalline structures. However, in the absence of *any* reversibility, the kinetic product is likely to be amorphous.

Finally, processes like Ostwald ripening or digestive ripening suggest that even in strongly bonded systems, the monomer must be able to redissolve.[94] Here, the conditions will play a

pivotal role. At room temperature, in the absence of acid, strongly bonded systems might not be in chemical equilibrium, and are under kinetic control. At higher temperature, in the presence of surfactant and acid, dissolution of the nanocrystal core could become possible and the reaction becomes thermodynamically controlled. Perhaps, the different theories of nucleation and growth simply describe different experimental conditions.

5.3 Kinetic models of nucleation and growth

Finke *et al.* followed the path of traditional chemical kinetics to describe nanocrystal nucleation and growth.[14,80,95–97] In the case of Ir nanocrystals (synthesized by reducing an Ir complex with hydrogen), the precursor decomposition and particle formation kinetics could be described by an autocatalytic process, written very generally as

$$\mathrm{A} \longrightarrow \mathrm{B} \tag{14}$$

$$\mathrm{A} + \mathrm{B} \longrightarrow 2\,\mathrm{B} \tag{15}$$

where A is the precursor and B represents a nanocrystal. The first reaction is the slow conversion of the precursor. The second reaction is the precursor conversion catalyzed by the Ir nanocrystal itself. The overall conversion kinetics feature a sigmoidal shape typical for autocatalytic processes, see Figure 5. This two-step autocatalysis model uses minimal equations and the first equation is supposed to represent nucleation and the second one is recognized as growth. Note that each of these reactions are written as irreversible. Kinetic studies led to a detailed chemical equation for the first step.[95,96]

$$3(\mathrm{COD})\mathrm{Ir} \cdot \mathrm{POM}^{8-} + 7.5\mathrm{H}_2 \longrightarrow \mathrm{Ir}_3 + 3\,\mathrm{POM}^{9-} + 3\,\mathrm{H}^+ + 3\mathrm{C}_8\mathrm{H}_{16} \tag{16}$$

Here COD is 1,5–cyclooctadiene and POM is a polyoxometallate ($\mathrm{P_2W_{15}Nb_3O_{62}}^{9-}$). Equation 16 is termolecular but second order in the precursor ($(\mathrm{COD})\mathrm{Ir} \cdot \mathrm{POM}^{8-}$). The mecha-

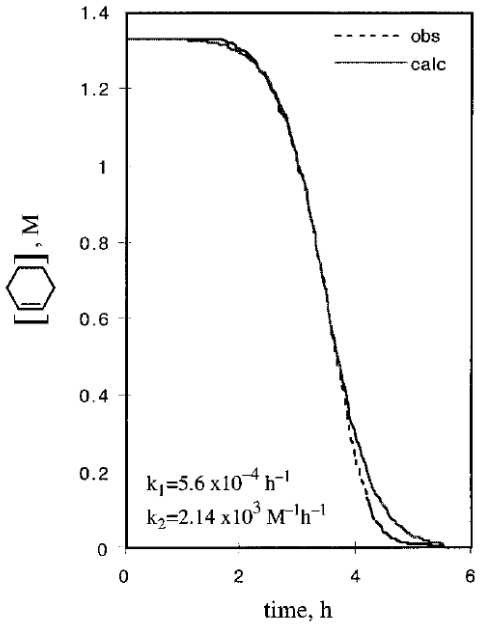

Figure 5: The conversion to Ir nanocrystals is monitored by a reporter reaction; reduction of cyclohexene. The typical sigmoidal curve of an autocatalytic process is observed. Reproduced from reference.[14] Copyright 1997 American Chemical Society.

nism consists of a pre–equilibrium and a second, rate–limiting step.

$$(\mathrm{COD})\mathrm{Ir} \cdot \mathrm{POM}^{8-} \overset{K_{diss}}{\rightleftharpoons} (\mathrm{COD})\mathrm{Ir}^{+} + 3\,\mathrm{POM}^{9-} \tag{17}$$

$$2(\mathrm{COD})\mathrm{Ir}^{+} + (\mathrm{COD})\mathrm{Ir} \cdot \mathrm{POM}^{8-} + 7.5\mathrm{H}_2 \xrightarrow{k} \mathrm{Ir}_3 + \mathrm{POM}^{9-} + 3\,\mathrm{H}^{+} + 3\mathrm{C}_8\mathrm{H}_{16} \tag{18}$$

Summing up Equations 17 and 18 yields Equation 16. From this chemically specific equation it is easier to recognize that the first step represents nucleation, with a nucleus size $n = 3$. This nucleus size is much smaller than proposed by CNT (>15). Here it is interesting to reflect on the definition of nucleation. The definition provided by CNT is related to the critical size where monomer attachment becomes favorable. The kinetically effective nucleus as defined by Finke is the first collection of atoms. One could however interpret the Ir_3 species as a soluble pre–nucleation cluster, much like the $\mathrm{Fe}_3\mathrm{O}$ precursor mentioned above.[81] A definition of a nucleus could be a particle that grows further and that contributes to the final number of particles (before Ostwald ripening). The balance between nucleation

and growth thus determines particle size. If the Ir_3 species grows further by reacting with precursor, it is a nucleus. If the Ir_3 species reacts with Ir_n particles to form Ir_{n+3}, it is solute.

The above 2–step model could adequately describe precursor conversion and total amount of Ir formed. However, it could not simulate the correct size distribution by population balance modelling.[97] The size distribution was much better described by adapting the 2–step model to a 3–step model, containing two growth steps where small particles grow with a higher rate constant than bigger particles. This approach is reminiscent of the size–dependent growth rate introduced in the thermodynamic models. In contrast to a continuous variation of the growth rate with size ($k(n) = k/r^n$), *Finke et al.* used a step function, defining a certain nanocrystal size where the growth rate constant abruptly changes. Such a step function is farther from reality but in general discontinuities should not be completely excluded (consider for example magic sized clusters).[98–101]

By treating the whole nanocrystal formation process as a set of chemical equations, one can easily build up the complexity of the model to include various effects. Karim *et al.* considered the binding of ligands to both the Pd precursor complex and the final Pd nanocrystals by writing.[89,102]

$$\mathrm{A} + \mathrm{L} \underset{k_{-1}}{\overset{k_1}{\rightleftharpoons}} \mathrm{AL} \tag{19}$$

$$\mathrm{A} \xrightarrow{k_2} \mathrm{B} \tag{20}$$

$$\mathrm{A} + \mathrm{B} \xrightarrow{k_3} 2\,\mathrm{B} \tag{21}$$

$$\mathrm{B} + \mathrm{L} \underset{k_{-4}}{\overset{k_4}{\rightleftharpoons}} \mathrm{BL} \tag{22}$$

From their data and kinetic modeling, the authors were actually the first to conclude that larger particles grow slower than smaller particles, an effect they attributed to (i) a lower intrinsic surface reactivity for larger particles and (ii) a higher ligand coverage on larger particles.[89,102]

5.4 A chemically specific approach

The kinetics models do not feature a concept like a *critical concentration*. They do not invoke a supersaturation ratio. The nucleus is simply the first collection of atoms that is formed kinetically. At first sight, these models are also incompatible with independent precursor to monomer conversion since all the kinetic models feature autocatalytic precursor conversion. However, one could adapt Equation 8 to

$$\mathrm{P} \xrightarrow{k_1} \mathrm{M} \tag{23}$$

$$2\,\mathrm{M} \xrightarrow{k_{2n}} \mathrm{M}_2 \tag{24}$$

$$3\,\mathrm{M} \xrightarrow{k_{3n}} \mathrm{M}_3 \tag{25}$$

$$\mathrm{M} + \mathrm{M}_2 \xrightarrow{k_3} \mathrm{M}_3 \tag{26}$$

$$\mathrm{M} + \mathrm{M}_3 \xrightarrow{k_4} \mathrm{M}_3 \tag{27}$$

$$\mathrm{M} + \mathrm{M}_4 \xrightarrow{k_5} \mathrm{M}_5 \tag{28}$$

The first step is precursor conversion. The second and third are either bimolecular or termolecular nucleation. The other steps represent growth. Instead of writing minimal equations, every reaction is explicitly written. This way of representing nanocrystal formation could potentially give a lot of insight and combine the features of different models. One can further refine this approach by considering ligand binding or the aggregation of smaller particles. One could also make every reaction reversible (thermodynamic control). Size–dependent growth kinetics are easily introduced by taking: $k_3 > k_4 > k_5 > ....$ Magic size clusters of size n can be rationalized as a discontinuity in this series: $k_{n-1} > k_n >>> k_{n+1} < k_{n+2} > k_{n+3} > ....$ We can also rationalize how to steer the balance between nucleation and growth (and thus tune particle size). The bimolecular nucleation rate is

$$v_{nucl} = k_{2n}[M]^2 \tag{29}$$

The growth rate is

$$v_{growth} = \sum_{n>2} k_n[M][M_{n-1}] = [M] \sum_{n>2} k_n[M_{n-1}] \tag{30}$$

The nucleation rate is second order in the monomer concentration, while the growth rate is first order. A high monomer concentration will thus favor nucleation, while a low monomer concentration will favor growth. This is an alternative explanation to the relation between precursor conversion rate and particle number. A high precursor conversion rate will cause a high monomer concentration, thus favoring nucleation over growth. In contrast, the addition of ligand was reported to promote growth over nucleation, which is particularly important in a seeded growth reaction (where one aims to avoid nucleation).[103] This observation can be understood within the above set of chemical equations by adding a monomer–ligand equilibrium.

$$\mathrm{M + L \rightleftharpoons ML} \tag{31}$$

By adding ligand, the effective concentration of uncoordinated monomer is decreased (by shifting the equilibrium to coordinated monomer). A lower monomer concentration favors growth over nucleation because of the difference in kinetic order.

While this approach could potentially unite various aspects of both thermodynamic and kinetics models, and aims at explicitly addressing the chemical reactions underlying a nanocrystal reaction, it is also inherently flawed since it still relies on the concept of the monomer. Instead of defining the monomer as a single unit of the nanocrystal, one could also define it as the species directly preceding the nucleation reaction.[104] For example, in the case of PbS we showed that the $(PbS)_2$ dimer is the soluble species formed by precursor conversion. Perhaps, we should replace M in the above equations by this dimer. There might also be reactions that never form a solute (as for example proposed by the model of Finke *et al.*). Other reactions proceed through coordination polymers or mesophase intermediates, further challenging the above approach.[26,105]

As scientists we are often tempted to over–generalize. However, it is hard to conceive that there is a single theory that can describe the synthesis of zirconia nanocrystals at 340 °C, and the synthesis of catalytic Ir nanocrystals at 22 °C, and the synthesis of PbS nanocrystals at 120 °C. Even small differences in the precursor chemistry can change the mechanism. For example, magic sized clusters have been clearly identified in the synthesis of InP nanocrystals from indium carboxylate precursors while these have not (yet) been observed when starting from indium halide precursors.[106] When studying the chemistry of nucleation, we should thus not reduce the problem to an abstract monomer but one needs to take into account the specific chemical nature of the species. This requires detailed investigation of the coordination chemistry of precursors and their exact decomposition mechanism.[29,38,43,78,107–109] Such studies benefit greatly from x-ray based (synchrotron) techniques, e.g., small angle x-ray scattering (SAXS), extended x-ray absorption fine structure (EXAFS) spectroscopy and pair distribution function (PDF) analysis.[88,104,110]

We are still very far from a retro–synthetic analysis of nanocrystals, but we have made important progress in recent years. We dismissed burst nucleation, introduced superfocusing and are starting to look into the fine chemical details of nanocrystal synthesis.

6 Good chemical practice in nanocrystal synthesis

As we discussed in this perspective, nanocrystal formation is a series of chemical reactions. A chemical reaction is conveniently described by a chemical equation, see Scheme 7. It would thus be very helpful to the nanochemist if every manuscript, which contains nanocrystal synthesis, presented a chemical equation to the reader. This is common practice in organic chemistry since a chemical equation is a very concise and efficient way of providing synthetic conditions to the reader. Ideally, this chemical equation is completely balanced, forcing the nanochemist to consider all by–products. However, the attentive reader will notice that even in this perspective not all chemical equations are fully balanced (in case the by–products are

unknown). Reporting the yield of a reaction is another habit in organic synthesis. It is an important metric to judge the efficiency of a certain synthetic strategy. There is no reason why a nanocrystal synthesis should be any different.

Writing chemical equations and reporting yields are basic recommendations for the nanochemist. In the following we discuss a few more aspects of good chemical practice; reagent purity and product purity. Other recommendations for reporting on the composition, size distribution, shape distribution, nanocrystal concentration and dopant concentration have been formulated in an editorial of Murphy and Buriak.[111]

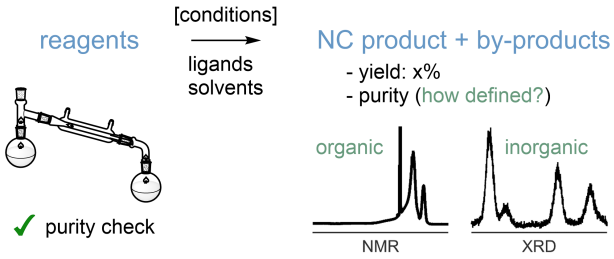

Scheme 7: Good chemical practice means writing down a balanced chemical equation, reporting the yield, and caring about reagent and product purity.

6.1 Purity of reagents

A truly robust and selective chemical reaction should be able to handle a couple of impurities. However, when a chemical reaction is as complicated as a nanocrystal synthesis, it is good practice to avoid adding external complexity. Impurities in reagents can exhibit side reactions, inhibit or accelerate nanocrystal growth, or steer anisotropic growth. For example, (di)alkylphosphinic acid and alkylphosphonic acid impurities in TOPO were shown to change the shape of the CdSe nanocrystals. The concentration of these impurities showed a large bath–to–batch variation. To achieve reproducible results, it is recommended to recrystallize TOPO before use.[112,113] The nanochemist can subsequently add a controlled amount of co–surfactant to the reaction. As a second example, oleylamine contains several impurities that reduce its capacity to dissolve salts.[114] Purification as a salt and subsequent vacuum

distillation is recommended. Furthermore, the use of technical oleylamine, with a varying blend of *cis*, *trans* and saturated chains, creates irreproducibility in the ligand shell structure, with implications on nanocrystal assembly and its use is not recommended for certain applications.[115] Oleylamine and TOPO received quite some attention because they are commonly used ligands. However, there can be impurities in every reagent that is used, including metal precursors and other organic molecules.[32] Techniques such as vacuum distillation and recrystallization should thus be part of the nanochemist's skill set. It is good chemical practise to perform some type of check of the reagents before use. For organic molecules one can easily take a ^{1}H NMR (and ^{31}P NMR) measurement before use.

6.2 Purity of nanocrystal products

After this complex reaction, the nanochemist has obtained the desired nanocrystals, together with large amounts of by–products, side–products, excess ligand and high–boiling solvent. While everyones agree that pure samples are a joy to work with, there are several unresolved issues in this regard. First, how does one define nanocrystal purity? Second, how does one go about proving the nanocrystal sample is pure? Third, should we as a community agree on a standard of reporting?

The easiest definition of nanocrystal purity is the one where one defines the bound ligands and the nanocrystal core as a single object and one declares all other species (by–products, free ligands, etc) as impurities. This definition works well for nanocrystals with a monolayer of tightly bound ligands but is less straightforward for ligands in dynamic exchange.[116] In addition, are all nanocrystals equal? Most certainly not, nanocrystals are typically a heterogeneous bunch.[72,117] Certainly in case of anisotropic nanocrystals, shape purity becomes an issue. Furthermore, one can think of crystal phase purity (anatase vs. rutile TiO_2), size dispersion (monodisperse vs. polydisperse), ligand purity (e.g., a mixture of ligands on the surface). Usually, the aim of the nanochemist or the intended application will determine the level and type of purity that is required.

Given the complex nature of nanocrystal purity, different purification techniques and analysis techniques have been developed. The various techniques of purification have been thoroughly reviewed by Greytak et al.[118] To report nanocrystal size, transmission electron microscopy (TEM) is frequently used. Only a small number of particles is usually counted and user bias (conscious or unconcious) is another serious problem. In case of non-spherical nanocrystals, the area is often converted into a diameter, using the formula of a circle. This approximation is acceptable as long as one is clear about the data processing and if the nanochemist recognizes that the resulting value for the "diameter" is only a rough estimation of the size. For cubic shapes, the cube edge length should be reported. Regarding size dispersion, we often fit a gaussian curve to a histogram and report mean μ and standard deviation σ. The size dispersion is then calculated as σ/μ, and expressed in percent. We are thus implicitly using the 68% confidence interval. By using an error of 2σ, we would be reporting in the 95 % confidence interval, which would be a step up in accuracy of reporting. Ensemble techniques like UV-Vis, SAXS and DLS (dynamic light scattering) probe the nanocrystal ensemble as a whole and are most representative.[119,120] Regarding crystal phase purity, X-ray diffraction (XRD) is a useful technique, especially when combined with Rietveld refinement.[121] While XRD is easily interpreted for relatively large nanocrystals, total X-ray scattering (and Pair Distribution Function (PDF) analysis) is recommended below a diameter of 5 nm, due to the broadening of the reflections in XRD.[122,123] Proton NMR spectroscopy allows the nanochemist to differentiate free from bound ligands based on the NMR line width,[124] and to detect any other type of organic impurity. Detailed NMR investigations can also differentiate a homogeneous ligand shell from a mixture of ligands.[62]

In any field, reproducibility stands or falls with the experimental section of a paper. In organic chemistry, there is a consensus on reporting the purification procedure and on the standard characterization. In the field of colloidal nanocrystals, the purification procedure is often described very succinctly, e.g., "precipitation with acetone and redispersion in toluene". For optimal reproducibility, it would be extremely helpful to report exact volumes

of antisolvent and solvent. In addition, proof should be provided that all by–products have been removed. A simple ^{1}H NMR spectrum seems the minimum characterization required to assess nanocrystal purity. It would be useful to come together as a field and discuss standard characterization techniques and standardized reporting for nanocrystal synthesis. Standardization will be particularly welcomed by computational chemists aiming at developing machine learning algorithms or by databases that need to mine scientific papers for data. While defining the standard characterization techniques, one should keep in mind that some techniques are not readily available to every nanochemist (requiring expensive instruments or synchrotron access). A balance needs to be sought.

7 Conclusion and outlook

The chemistry of colloidal nanocrystals has greatly advanced since the seminal paper of Bawendi *et al.* In this perspective, we analyzed the three components of colloidal synthesis: precursors, ligands, and solvent. Precursor chemistry has been thoroughly studied for some systems while others have received less attention. More efforts need to go in this direction since these chemical mechanisms will be the basis for a full retro–synthetic analysis of nanocrystal synthesis. Insight in the precursor conversion mechanism have a direct impact on the versatility and tunability of synthetic procedures. Recently, we found that also ligands often transform during nanocrystals synthesis. The nanochemist can thus not trust that the initial ligand added to the flask, is also the final ligand bound to the nanocrystal surface. It is recommended to explicitly analyze the surface chemistry of the nanocrystal product. The solvent is added to dilute the reagents and serve as a heat transfer medium. However, nanocrystal syntheses happen at such high temperatures that side reactions of the solvent cannot be excluded and we discussed here the example of 1-octadecene.

It is fair to say that the mechanism of nanocrystal crystallization (nucleation and growth) is still hotly debated and there exist various models in the literature. Some of these are based

on chemical reversibility (thermodynamic control) while others consider only the forward reaction (kinetic control). We introduced the idea here that these different models are perhaps describing different experimental conditions and are not fundamentally at odds with one another. Regardless of the model, there is a consensus that nucleation does not happen in a burst, as initially hypothesized by LaMer in 1950. Instead, continuous nucleation produces particles over a large portion of the reaction time. The still monodisperse outcome of the reaction is explained by strongly size–dependent growth kinetics. Another consensus is found in the recommendation for seeded–growth. To avoid nucleation and promote growth of the seed, a low precursor/monomer concentration is desired. A fully comprehensive mechanism of nanocrystal formation is still lacking though. It is very likely that different types of nanocrystals grow according to different mechanisms so a truly universal mechanism is unlikely to emerge and one should take into account the specific chemistry of the materials. More attention should go to the coordination chemistry of metal precursors and the initial complexes or clusters formed by precursor decomposition.

We reflected on good chemical practise for colloidal synthesis. All nanochemists are encouraged to write down chemical equations for their reactions and to report the yield of the reaction. Standard chemical purification techniques (distillation, recrystallization) should be taught to all nanochemists since impure chemicals will further complicate an already complicated chemical reaction. Finally, it seems not easy to define nanocrystal purity. This perspective is not meant as a final conclusion, but is hopefully the start of a constructive debate in the community. What is the minimum characterization required to report on a new nanocrystal synthesis? In how much detail should the purification be described in the experimental section? These are some of the questions we need to find an answer for.

The future is bright for nanochemistry. We have the chance of becoming a mature field that keeps pushing the boundaries of mechanistic insight and structural complexity of the products. The aspirations of many researchers in the field towards total nanosynthesis and

retro–synthetic analysis, is truly inspirational.

Acknowledgement

The author thanks the University of Basel for financial support.

References

(1) Murray, C. B.; Norris, D. J.; Bawendi, M. G. Synthesis and characterization of nearly monodisperse CdE (E = S, Se, Te) semiconductor nanocrystallites. *Journal of the American Chemical Society* **1993**, *115*, 8706–8715.

(2) Turkevich, J.; Stevenson, P. C.; Hillier, J. A study of the nucleation and growth processes in the synthesis of colloidal gold. *Discussions of the Faraday Society* **1951**, *11*, 55–75.

(3) Park, J.; Joo, J.; Kwon, S.; Jang, Y.; Hyeon, T. Synthesis of Monodisperse Spherical Nanocrystals. *Angewandte Chemie International Edition* **2007**, *46*, 4630–4660.

(4) Xia, Y.; Xiong, Y.; Lim, B.; Skrabalak, S. E. Shape-controlled synthesis of metal nanocrystals: simple chemistry meets complex physics? *Angewandte Chemie International Edition* **2009**, *48*, 60–103.

(5) Buonsanti, R.; Milliron, D. J. Chemistry of Doped Colloidal Nanocrystals. *Chemistry of Materials* **2013**, *25*, 1305–1317.

(6) Buck, M. R.; Schaak, R. E. Emerging Strategies for the Total Synthesis of Inorganic Nanostructures. *Angewandte Chemie International Edition* **2013**, *52*, 6154–6178.

(7) Garcia-Rodriguez, R.; Hendricks, M. P.; Cossairt, B. M.; Liu, H. T.; Owen, J. S. Conversion Reactions of Cadmium Chalcogenide Nanocrystal Precursors. *Chemistry of Materials* **2013**, *25*, 1233–1249.

(8) Efros, A. L.; Brus, L. E. Nanocrystal Quantum Dots: From Discovery to Modern Development. *ACS Nano* **2021**, *15*, 6192.

(9) Baek, W.; Chang, H.; Bootharaju, M. S.; Kim, J. H.; Park, S.; Hyeon, T. Recent Advances and Prospects in Colloidal Nanomaterials. *JACS Au* **2021**, *1*, 1849–1859.

(10) Battaglia, D.; Peng, X. Formation of High Quality InP and InAs Nanocrystals in a Noncoordinating Solvent. *Nano Letters* **2002**, *2*, 1027–1030.

(11) Lounis, S. D.; Runnerstrom, E. L.; Bergerud, A.; Nordlund, D.; Milliron, D. J. Influence of Dopant Distribution on the Plasmonic Properties of Indium Tin Oxide Nanocrystals. *Journal of the American Chemical Society* **2014**, *136*, 7110–7116.

(12) Niederberger, M.; Bartl, M. H.; Stucky, G. D. Benzyl Alcohol and Transition Metal Chlorides as a Versatile Reaction System for the Nonaqueous and Low-Temperature Synthesis of Crystalline Nano-Objects with Controlled Dimensionality. *Journal of the American Chemical Society* **2002**, *124*, 13642–13643.

(13) Joo, J.; Yu, T.; Kim, Y. W.; Park, H. M.; Wu, F.; Zhang, J. Z.; Hyeon, T. Multigram Scale Synthesis and Characterization of Monodisperse Tetragonal Zirconia Nanocrystals. *Journal of the American Chemical Society* **2003**, *125*, 6553–6557.

(14) Watzky, M. A.; Finke, R. G. Transition Metal Nanocluster Formation Kinetic and Mechanistic Studies. A New Mechanism When Hydrogen Is the Reductant: Slow, Continuous Nucleation and Fast Autocatalytic Surface Growth. *Journal of the American Chemical Society* **1997**, *119*, 10382–10400.

(15) Pery, T.; Pelzer, K.; Buntkowsky, G.; Philippot, K.; Limbach, H.-H.; Chaudret, B. Direct NMR Evidence for the Presence of Mobile Surface Hydrides on Ruthenium Nanoparticles. *ChemPhysChem* **2005**, *6*, 605–607.

(16) He, M.; Protesescu, L.; Caputo, R.; Krumeich, F.; Kovalenko, M. V. A General Synthesis Strategy for Monodisperse Metallic and Metalloid Nanoparticles (In, Ga, Bi, Sb, Zn, Cu, Sn, and Their Alloys) via in Situ Formed Metal Long-Chain Amides. *Chemistry of Materials* **2015**, *27*, 635–647.

(17) Boyer, J.-C.; Vetrone, F.; Cuccia, L. A.; Capobianco, J. A. Synthesis of Colloidal Upconverting NaYF4 Nanocrystals Doped with Er3+, Yb3+ and Tm3+, Yb3+ via Thermal Decomposition of Lanthanide Trifluoroacetate Precursors. *Journal of the American Chemical Society* **2006**, *128*, 7444–7445.

(18) Protesescu, L.; Yakunin, S.; Bodnarchuk, M. I.; Krieg, F.; Caputo, R.; Hendon, C. H.; Yang, R. X.; Walsh, A.; Kovalenko, M. V. Nanocrystals of Cesium Lead Halide Perovskites (CsPbX3, X = Cl, Br, and I): Novel Optoelectronic Materials Showing Bright Emission with Wide Color Gamut. *Nano Letters* **2015**, *15*, 3692–3696.

(19) Murray, C. B.; Kagan, C. R.; Bawendi, M. G. Self-Organization of CdSe Nanocrystallites into Three-Dimensional Quantum Dot Superlattices. *Science* **1995**, *270*, 1335–1338.

(20) Papadas, I. T.; Vamvasakis, I.; Tamiolakis, I.; Armatas, G. S. Templated Self-Assembly of Colloidal Nanocrystals into Three-Dimensional Mesoscopic Structures: A Perspective on Synthesis and Catalytic Prospects. *Chemistry of Materials* **2016**, *28*, 2886–2896.

(21) Cargnello, M. Colloidal Nanocrystals as Building Blocks for Well-Defined Heterogeneous Catalysts. *Chemistry of Materials* **2019**, *31*, 576–596.

(22) Huang, J.; Buonsanti, R. Colloidal Nanocrystals as Heterogeneous Catalysts for Electrochemical CO2 Conversion. *Chemistry of Materials* **2019**, *31*, 13–25.

(23) Oszajca, M. F.; Bodnarchuk, M. I.; Kovalenko, M. V. Precisely Engineered Colloidal

Nanoparticles and Nanocrystals for Li-Ion and Na-Ion Batteries: Model Systems or Practical Solutions? *Chemistry of Materials* **2014**, *26*, 5422–5432.

(24) Yang, J.; Choi, M. K.; Yang, U. J.; Kim, S. Y.; Kim, Y. S.; Kim, J. H.; Kim, D.-H.; Hyeon, T. Toward Full-Color Electroluminescent Quantum Dot Displays. *Nano Letters* **2021**, *21*, 26–33.

(25) Bang, S. Y.; Suh, Y.-H.; Fan, X.-B.; Shin, D.-W.; Lee, S.; Choi, H. W.; Lee, T. H.; Yang, J.; Zhan, S.; Harden-Chaters, W.; Samarakoon, C.; Occhipinti, L. G.; Han, S. D.; Jung, S.-M.; Kim, J. M. Technology progress on quantum dot light-emitting diodes for next-generation displays. *Nanoscale Horizons* **2021**, *6*, 68–77.

(26) Loiudice, A.; Buonsanti, R. Reaction intermediates in the synthesis of colloidal nanocrystals. *Nature synthesis* **2022**, *1*, 344–351.

(27) Ojea-Jiménez, I.; Romero, F. M.; Bastús, N. G.; Puntes, V. Small Gold Nanoparticles Synthesized with Sodium Citrate and Heavy Water: Insights into the Reaction Mechanism. *The Journal of Physical Chemistry C* **2010**, *114*, 1800–1804.

(28) Whitehead, C. B.; Finke, R. G. Nucleation Kinetics and Molecular Mechanism in Transition-Metal Nanoparticle Formation: The Intriguing, Informative Case of a Bimetallic Precursor, [(1,5-COD)IrI·HPO4]22–. *Chemistry of Materials* **2019**, *31*, 2848–2862.

(29) Strach, M.; Mantella, V.; Pankhurst, J. R.; Iyengar, P.; Loiudice, A.; Das, S.; Corminboeuf, C.; van Beek, W.; Buonsanti, R. Insights into Reaction Intermediates to Predict Synthetic Pathways for Shape-Controlled Metal Nanocrystals. *Journal of the American Chemical Society* **2019**, *141*, 16312–16322.

(30) Vivien, A.; Guillaumont, M.; Meziane, L.; Salzemann, C.; Aubert, C.; Halbert, S.; Gérard, H.; Petit, M.; Petit, C. Role of Oleylamine Revisited: An Original Dispro-

portionation Route to Monodispersed Cobalt and Nickel Nanocrystals. *Chemistry of Materials* **2019**, *31*, 960–968.

(31) Liu, H. T.; Owen, J. S.; Alivisatos, A. P. Mechanistic study of precursor evolution in colloidal group II-VI semiconductor nanocrystal synthesis. *Journal of the American Chemical Society* **2007**, *129*, 305–312.

(32) Frenette, L. C.; Krauss, T. D. Uncovering active precursors in colloidal quantum dot synthesis. *Nature Communications* **2017**, *8*, 2082.

(33) Hamachi, L. S.; Plante, I. J. L.; Coryell, A. C.; De Roo, J.; Owen, J. S. Kinetic Control over CdS Nanocrystal Nucleation Using a Library of Thiocarbonates, Thiocarbamates, and Thioureas. *Chemistry of Materials* **2017**, *29*, 8711–8719.

(34) Campos, M. P.; Hendricks, M. P.; Beecher, A. N.; Walravens, W.; Swain, R. A.; Cleveland, G. T.; Hens, Z.; Sfeir, M. Y.; Owen, J. S. A Library of Selenourea Precursors to PbSe Nanocrystals with Size Distributions near the Homogeneous Limit. *Journal of the American Chemical Society* **2017**, *139*, 2296–2305.

(35) Sowers, K. L.; Swartz, B.; Krauss, T. D. Chemical Mechanisms of Semiconductor Nanocrystal Synthesis. *Chemistry of Materials* **2013**, *25*, 1351–1362.

(36) Niederberger, M.; Garnweitner, G. Organic Reaction Pathways in the Nonaqueous Synthesis of Metal Oxide Nanoparticles. *Chemistry - a European Journal* **2006**, *12*, 7282–302.

(37) Ito, D.; Yokoyama, S.; Zaikova, T.; Masuko, K.; Hutchison, J. E. Synthesis of Ligand-Stabilized Metal Oxide Nanocrystals and Epitaxial Core/Shell Nanocrystals via a Lower-Temperature Esterification Process. *ACS Nano* **2014**, *8*, 64–75.

(38) Pokratath, R.; Van den Eynden, D.; Cooper, S. R.; Mathiesen, J. K.; Waser, V.; Devereux, M.; Billinge, S. J. L.; Meuwly, M.; Jensen, K. M. .; De Roo, J. Mechanistic

Insight into the Precursor Chemistry of ZrO2 and HfO2 Nanocrystals; towards Size-Tunable Syntheses. *JACS Au* **2022**, *2*, 827.

(39) Imran, M.; Caligiuri, V.; Wang, M.; Goldoni, L.; Prato, M.; Krahne, R.; De Trizio, L.; Manna, L. Benzoyl Halides as Alternative Precursors for the Colloidal Synthesis of Lead-Based Halide Perovskite Nanocrystals. *Journal of the American Chemical Society* **2018**, *140*, 2656–2664.

(40) Tessier, M. D.; De Nolf, K.; Dupont, D.; Sinnaeve, D.; De Roo, J.; Hens, Z. Aminophosphines: A Double Role in the Synthesis of Colloidal Indium Phosphide Quantum Dots. *Journal of the American Chemical Society* **2016**, *138*, 5923–5929.

(41) Grigel, V.; Dupont, D.; De Nolf, K.; Hens, Z.; Tessier, M. D. InAs Colloidal Quantum Dots Synthesis via Aminopnictogen Precursor Chemistry. *Journal of the American Chemical Society* **2016**, *138*, 13485–13488.

(42) Chen, Y.; Landes, N. T.; Little, D. J.; Beaulac, R. Conversion Mechanism of Soluble Alkylamide Precursors for the Synthesis of Colloidal Nitride Nanomaterials. *Journal of the American Chemical Society* **2018**, *140*, 10421.

(43) Parvizian, M.; Duràn Balsa, A.; Pokratath, R.; Kalha, C.; Lee, S.; Ibanez, M.; Regoutz, A.; De Roo, J. The chemistry of Cu3N and Cu3PdN nanocrystals. *ChemRxiv* **March 23, 2022**, DOI: 10.26434/chemrxiv–2022–2tjc0–v2.

(44) Song, W.-S.; Lee, H.-S.; Lee, J. C.; Jang, D. S.; Choi, Y.; Choi, M.; Yang, H. Amine-derived synthetic approach to color-tunable InP/ZnS quantum dots with high fluorescent qualities. *Journal of Nanoparticle Research* **2013**, *15*, 1750.

(45) Tessier, M. D.; Dupont, D.; De Nolf, K.; De Roo, J.; Hens, Z. Economic and Size-Tunable Synthesis of InP/ZnE (E = S, Se) Colloidal Quantum Dots. *Chemistry of Materials* **2015**, *27*, 4893–4898.

(46) Buffard, A.; Dreyfuss, S.; Nadal, B.; Heuclin, H.; Xu, X.; Patriarche, G.; Mézailles, N.; Dubertret, B. Mechanistic Insight and Optimization of InP Nanocrystals Synthesized with Aminophosphines. *Chemistry of Materials* **2016**, *28*, 5925–5934.

(47) Wu, H.; Chen, W. Copper nitride nanocubes: size-controlled synthesis and application as cathode catalyst in alkaline fuel cells. *Journal of the American Chemical Society* **2011**, *133*, 15236–9.

(48) Vaughn Ii, D. D.; Araujo, J.; Meduri, P.; Callejas, J. F.; Hickner, M. A.; Schaak, R. E. Solution Synthesis of Cu3PdN Nanocrystals as Ternary Metal Nitride Electrocatalysts for the Oxygen Reduction Reaction. *Chemistry of Materials* **2014**, *26*, 6226–6232.

(49) Lord, R. W.; Holder, C. F.; Fenton, J. L.; Schaak, R. E. Seeded Growth of Metal Nitrides on Noble-Metal Nanoparticles To Form Complex Nanoscale Heterostructures. *Chemistry of Materials* **2019**, *31*, 4605–4613.

(50) Yarur Villanueva, F.; Green, P. B.; Qiu, C.; Ullah, S. R.; Buenviaje, K.; Howe, J. Y.; Majewski, M. B.; Wilson, M. W. B. Binary Cu2–xS Templates Direct the Formation of Quaternary Cu2ZnSnS4 (Kesterite, Wurtzite) Nanocrystals. *ACS Nano* **2021**, *15*, 18085–18099.

(51) Man, R. W. Y.; Brown, A. R. C.; Wolf, M. O. Mechanism of Formation of Palladium Nanoparticles: Lewis Base Assisted, Low-Temperature Preparation of Monodisperse Nanoparticles. *Angewandte Chemie International Edition* **2012**, *51*, 11350–11353.

(52) Chen, Z.; Song, Y.; Cai, J.; Zheng, X.; Han, D.; Wu, Y.; Zang, Y.; Niu, S.; Liu, Y.; Zhu, J.; Liu, X.; Wang, G. Tailoring the d-Band Centers Enables Co4N Nanosheets To Be Highly Active for Hydrogen Evolution Catalysis. *Angewandte Chemie International Edition* **2018**, *57*, 5076–5080.

(53) Parvizian, M.; De Roo, J. Precursor chemistry of metal nitride nanocrystals. *Nanoscale* **2021**, *13*, 18865–18882.

(54) Yang, Y.; Qin, H.; Peng, X. Intramolecular Entropy and Size-Dependent Solution Properties of Nanocrystal–Ligands Complexes. *Nano Letters* **2016**, *16*, 2127–2132.

(55) Yang, Y.; Qin, H.; Jiang, M.; Lin, L.; Fu, T.; Dai, X.; Zhang, Z.; Niu, Y.; Cao, H.; Jin, Y.; Zhao, F.; Peng, X. Entropic Ligands for Nanocrystals: From Unexpected Solution Properties to Outstanding Processability. *Nano Lett.* **2016**, *16*, 2133–2138.

(56) Kister, T.; Monego, D.; Mulvaney, P.; Widmer-Cooper, A.; Kraus, T. Colloidal Stability of Apolar Nanoparticles: The Role of Particle Size and Ligand Shell Structure. *ACS Nano* **2018**, *12*, 5969–5977.

(57) Doblas, D.; Kister, T.; Cano-Bonilla, M.; González-García, L.; Kraus, T. Colloidal Solubility and Agglomeration of Apolar Nanoparticles in Different Solvents. *Nano Letters* **2019**, *19*, 5246–5252.

(58) Monego, D.; Kister, T.; Kirkwood, N.; Mulvaney, P.; Widmer-Cooper, A.; Kraus, T. Colloidal Stability of Apolar Nanoparticles: Role of Ligand Length. *Langmuir* **2018**, *34*, 12982–12989.

(59) Monego, D.; Kister, T.; Kirkwood, N.; Doblas, D.; Mulvaney, P.; Kraus, T.; Widmer-Cooper, A. When Like Destabilizes Like: Inverted Solvent Effects in Apolar Nanoparticle Dispersions. *ACS Nano* **2020**, *14*, 5278–5287.

(60) Pang, Z.; Zhang, J.; Cao, W.; Kong, X.; Peng, X. Partitioning surface ligands on nanocrystals for maximal solubility. *Nature Communications* **2019**, *10*, 2454.

(61) Mourdikoudis, S.; Liz-Marzan, L. M. Oleylamine in Nanoparticle Synthesis. *Chemistry of Materials* **2013**, *25*, 1465–1476.

(62) De Keukeleere, K.; Coucke, S.; De Canck, E.; Van Der Voort, P.; Delpech, F.; Coppel, Y.; Hens, Z.; Van Driessche, I.; Owen, J. S.; De Roo, J. Stabilization of Colloidal

Ti, Zr, and Hf Oxide Nanocrystals by Protonated Tri-n-octylphosphine Oxide (TOPO) and Its Decomposition Products. *Chemistry of Materials* **2017**, *29*, 10233–10242.

(63) Wolcott, A.; Fitzmorris, R. C.; Muzaffery, O.; Zhang, J. Z. CdSe Quantum Rod Formation Aided By In Situ TOPO Oxidation. *Chemistry of Materials* **2010**, *22*, 2814–2821.

(64) Calcabrini, M.; Van den Eynden, D.; Ribot, S. S.; Pokratath, R.; Llorca, J.; De Roo, J.; Ibáñez, M. Ligand Conversion in Nanocrystal Synthesis: The Oxidation of Alkylamines to Fatty Acids by Nitrate. *JACS Au* **2021**, *1*, 1898–1903.

(65) Peng, X. G.; Manna, L.; Yang, W. D.; Wickham, J.; Scher, E.; Kadavanich, A.; Alivisatos, A. P. Shape control of CdSe nanocrystals. *Nature* **2000**, *404*, 59–61.

(66) Carbone, L. et al. Synthesis and Micrometer-Scale Assembly of Colloidal CdSe/CdS Nanorods Prepared by a Seeded Growth Approach. *Nano Lett.* **2007**, *7*, 2942–2950.

(67) Dhaene, E.; Pokratath, R.; Aalling-Frederiksen, O.; Jensen, K. M. O.; Smet, P. F.; de Buysser, K.; de Roo, J. Mono-alkyl phosphinic acids as ligands in nanocrystal synthesis. *ACS Nano* **2022**, DOI: 10.1021/acsnano.1c08966.

(68) Drijvers, E.; De Roo, J.; Geiregat, P.; Fehér, K.; Hens, Z.; Aubert, T. Revisited Wurtzite CdSe Synthesis: A Gateway for the Versatile Flash Synthesis of Multishell Quantum Dots and Rods. *Chem. Mater.* **2016**, *28*, 7311–7323.

(69) Hendricks, M. P.; Campos, M. P.; Cleveland, G. T.; Jen-La Plante, I.; Owen, J. S. A tunable library of substituted thiourea precursors to metal sulfide nanocrystals. *Science* **2015**, *348*, 1226–1230.

(70) Dhaene, E.; Billet, J.; Bennett, E.; Van Driessche, I.; De Roo, J. The Trouble with ODE: Polymerization during Nanocrystal Synthesis. *Nano Letters* **2019**, *19*, 7411–7417.

(71) Gordon, T. R.; Cargnello, M.; Paik, T.; Mangolini, F.; Weber, R. T.; Fornasiero, P.; Murray, C. B. Nonaqueous Synthesis of TiO2 Nanocrystals Using TiF4 to Engineer Morphology, Oxygen Vacancy Concentration, and Photocatalytic Activity. *Journal of the American Chemical Society* **2012**, *134*, 6751–6761.

(72) Hens, Z.; De Roo, J. Atomically Precise Nanocrystals. *J Am Chem Soc* **2020**, *142*, 15627–15637.

(73) Scott, S. L. The Burden of Disproof. *ACS Catalysis* **2019**, *9*, 4706–4708.

(74) Abe, S.; Capek, R. K.; De Geyter, B.; Hens, Z. Tuning the postfocused size of colloidal nanocrystals by the reaction rate: from theory to application. *Acs Nano* **2012**, *6*, 42–53.

(75) Kwon, S. G.; Piao, Y.; Park, J.; Angappane, S.; Jo, Y.; Hwang, N. M.; Park, J. G.; Hyeon, T. Kinetics of monodisperse iron oxide nanocrystal formation by "heating-up" process. *Journal of the American Chemical Society* **2007**, *129*, 12571–12584.

(76) Finney, E. E.; Finke, R. G. The Four-Step, Double-Autocatalytic Mechanism for Transition-Metal Nanocluster Nucleation, Growth, and Then Agglomeration: Metal, Ligand, Concentration, Temperature, and Solvent Dependency Studies. *Chemistry of Materials* **2008**, *20*, 1956–1970.

(77) Thanh, N. T. K.; Maclean, N.; Mahiddine, S. Mechanisms of Nucleation and Growth of Nanoparticles in Solution. *Chemical Reviews* **2014**, *114*, 7610–7630.

(78) Campos, M. P.; De Roo, J.; Greenberg, M. W.; McMurtry, B. M.; Hendricks, M. P.; Bennett, E.; Saenz, N.; Sfeir, M. Y.; Abécassis, B.; Ghose, S. K.; Owen, J. S. Growth kinetics determine the polydispersity and size of PbS and PbSe nanocrystals. *Chemical Science* **2022**, *13*, 4555–4565.

(79) LaMer, V. K.; Dinegar, R. H. Theory, Production and Mechanism of Formation of Monodispersed Hydrosols. *Journal of the American Chemical Society* **1950**, *72*, 4847–4854.

(80) Whitehead, C. B.; Özkar, S.; Finke, R. G. LaMer's 1950 Model for Particle Formation of Instantaneous Nucleation and Diffusion-Controlled Growth: A Historical Look at the Model's Origins, Assumptions, Equations, and Underlying Sulfur Sol Formation Kinetics Data. *Chemistry of Materials* **2019**, *31*, 7116–7132.

(81) Chang, H. et al. Molecular-Level Understanding of Continuous Growth from Iron-Oxo Clusters to Iron Oxide Nanoparticles. *Journal of the American Chemical Society* **2019**, *141*, 7037–7045.

(82) Sugimoto, T. Underlying mechanisms in size control of uniform nanoparticles. *Journal of Colloid and Interface Science* **2007**, *309*, 106–118.

(83) Sugimoto, T.; Shiba, F.; Sekiguchi, T.; Itoh, H. Spontaneous nucleation of monodisperse silver halide particles from homogeneous gelatin solution I: silver chloride. *Colloids and Surfaces A: Physicochemical and Engineering Aspects* **2000**, *164*, 183–203.

(84) Chu, D. B. K.; Owen, J. S.; Peters, B. Nucleation and Growth Kinetics from LaMer Burst Data. *The Journal of Physical Chemistry A* **2017**, *121*, 7511–7517.

(85) Bennett, E.; Greenberg, M. W.; Jordan, A. J.; Hamachi, L. S.; Banerjee, S.; Billinge, S. J. L.; Owen, J. S. Size Dependent Optical Properties and Structure of ZnS Nanocrystals Prepared from a Library of Thioureas. *Chemistry of Materials* **2022**, *34*, 706–717.

(86) Owen, J. S.; Chan, E. M.; Liu, H.; Alivisatos, A. P. Precursor Conversion Kinetics and the Nucleation of Cadmium Selenide Nanocrystals. *Journal of the American Chemical Society* **2010**, *132*, 18206–18213.

(87) Talapin, D. V.; Rogach, A. L.; Haase, M.; Weller, H. Evolution of an Ensemble of Nanoparticles in a Colloidal Solution: Theoretical Study. *The Journal of Physical Chemistry B* **2001**, *105*, 12278–12285.

(88) Whitehead, C. B.; Finke, R. G. Particle formation mechanisms supported by in situ synchrotron XAFS and SAXS studies: a review of metal, metal-oxide, semiconductor and selected other nanoparticle formation reactions. *Material Advances* **2021**, *2*, 6532–6568.

(89) Mozaffari, S.; Li, W.; Thompson, C.; Ivanov, S.; Seifert, S.; Lee, B.; Kovarik, L.; Karim, A. M. Colloidal nanoparticle size control: experimental and kinetic modeling investigation of the ligand–metal binding role in controlling the nucleation and growth kinetics. *Nanoscale* **2017**, *9*, 13772–13785.

(90) Prins, P. T. et al. Extended Nucleation and Superfocusing in Colloidal Semiconductor Nanocrystal Synthesis. *Nano Letters* **2021**, *21*, 2487.

(91) McMurtry, B. M.; Qian, K.; Teglasi, J. K.; Swarnakar, A. K.; De Roo, J.; Owen, J. S. Continuous Nucleation and Size Dependent Growth Kinetics of Indium Phosphide Nanocrystals. *Chemistry of Materials* **2020**, *32*, 4358–4368.

(92) Whitehead, C. B.; Özkar, S.; Finke, R. G. LaMer's 1950 model of particle formation: a review and critical analysis of its classical nucleation and fluctuation theory basis, of competing models and mechanisms for phase-changes and particle formation, and then of its application to silver halide, semiconductor, metal, and metal-oxide nanoparticles. *Materials Advances* **2021**, *2*, 186–235.

(93) Srivastava, V.; Kamysbayev, V.; Hong, L.; Dunietz, E.; Klie, R. F.; Talapin, D. V. Colloidal Chemistry in Molten Salts: Synthesis of Luminescent In1- xGa xP and In1- xGa xAs Quantum Dots. *Journal of the American Chemical Society* **2018**, *140*, 12144–12151.

(94) Razgoniaeva, N.; Yang, M.; Garrett, P.; Kholmicheva, N.; Moroz, P.; Eckard, H.; Royo Romero, L.; Porotnikov, D.; Khon, D.; Zamkov, M. Just Add Ligands: Self-Sustained Size Focusing of Colloidal Semiconductor Nanocrystals. *Chemistry of Materials* **2018**, *30*, 1391–1398.

(95) Laxson, W. W.; Finke, R. G. Nucleation is Second Order: An Apparent Kinetically Effective Nucleus of Two for Ir(0)n Nanoparticle Formation from [(1,5-COD)IrI·P2W15Nb3O62]8– Plus Hydrogen. *Journal of the American Chemical Society* **2014**, *136*, 17601–17615.

(96) Özkar, S.; Finke, R. G. Nanoparticle Nucleation Is Termolecular in Metal and Involves Hydrogen: Evidence for a Kinetically Effective Nucleus of Three Ir3H2x·P2W15Nb3O626– in Ir(0)n Nanoparticle Formation From [(1,5-COD)IrI·P2W15Nb3O62]8– Plus Dihydrogen. *Journal of the American Chemical Society* **2017**, *139*, 5444–5457.

(97) Handwerk, D. R.; Shipman, P. D.; Whitehead, C. B.; Özkar, S.; Finke, R. G. Mechanism-Enabled Population Balance Modeling of Particle Formation en Route to Particle Average Size and Size Distribution Understanding and Control. *Journal of the American Chemical Society* **2019**, *141*, 15827–15839.

(98) Gary, D. C.; Terban, M. W.; Billinge, S. J. L.; Cossairt, B. M. Two-Step Nucleation and Growth of InP Quantum Dots via Magic-Sized Cluster Intermediates. *Chemistry of Materials* **2015**, *27*, 1432–1441.

(99) Beecher, A. N.; Yang, X.; Palmer, J. H.; LaGrassa, A. L.; Juhas, P.; Billinge, S. J. L.; Owen, J. S. Atomic Structures and Gram Scale Synthesis of Three Tetrahedral Quantum Dots. *Journal of the American Chemical Society* **2014**, *136*, 10645–10653.

(100) Pun, A. B.; Mule, A. S.; Held, J. T.; Norris, D. J. Core/Shell Magic-Sized CdSe Nanocrystals. *Nano Letters* **2021**, *21*, 7651–7658.

(101) Sakthivel, N. A.; Dass, A. Aromatic Thiolate-Protected Series of Gold Nanomolecules and a Contrary Structural Trend in Size Evolution. *Accounts of Chemical Research* **2018**, *51*, 1774–1783.

(102) Mozaffari, S.; Li, W.; Dixit, M.; Seifert, S.; Lee, B.; Kovarik, L.; Mpourmpakis, G.; Karim, A. M. The role of nanoparticle size and ligand coverage in size focusing of colloidal metal nanoparticles. *Nanoscale Advances* **2019**, *1*, 4052–4066.

(103) Nakonechnyi, I.; Sluydts, M.; Justo, Y.; Jasieniak, J.; Hens, Z. Mechanistic Insights in Seeded Growth Synthesis of Colloidal Core/Shell Quantum Dots. *Chemistry of Materials* **2017**, *29*, 4719–4727.

(104) Koziej, D. Revealing Complexity of Nanoparticle Synthesis in Solution by in Situ Hard X-ray Spectroscopy—Today and Beyond. *Chemistry of Materials* **2016**, *28*, 2478–2490.

(105) Mantella, V.; Strach, M.; Frank, K.; Pankhurst, J. R.; Stoian, D.; Gadiyar, C.; Nickel, B.; Buonsanti, R. Polymer Lamellae as Reaction Intermediates in the Formation of Copper Nanospheres as Evidenced by In Situ X-ray Studies. *Angewandte Chemie International Edition* **2020**, *59*, 11627–11633.

(106) Cossairt, B. M. Shining Light on Indium Phosphide Quantum Dots: Understanding the Interplay among Precursor Conversion, Nucleation, and Growth. *Chemistry of Materials* **2016**, *28*, 7181–7189.

(107) Jensen, G. V.; Bremholm, M.; Lock, N.; Deen, G. R.; Jensen, T. R.; Iversen, B. B.; Niederberger, M.; Pedersen, J. S.; Birkedal, H. Anisotropic Crystal Growth Kinetics of Anatase TiO2 Nanoparticles Synthesized in a Nonaqueous Medium. *Chemistry of Materials* **2010**, *22*, 6044–6055.

(108) Dippel, A.-C.; Jensen, K. M. O.; Tyrsted, C.; Bremholm, M.; Bojesen, E. D.; Saha, D.; Birgisson, S.; Christensen, M.; Billinge, S. J. L.; Iversen, B. B. Towards atomistic

understanding of polymorphism in the solvothermal synthesis of ZrO2 nanoparticles. *Acta Crystallographica Section A* **2016**, *72*, 645–650.

(109) Anker, A. S.; Christiansen, T. L.; Weber, M.; Schmiele, M.; Brok, E.; Kjær, E. T. S.; Juhás, P.; Thomas, R.; Mehring, M.; Jensen, K. M. . Structural Changes during the Growth of Atomically Precise Metal Oxido Nanoclusters from Combined Pair Distribution Function and Small-Angle X-ray Scattering Analysis. *Angewandte Chemie International Edition* **2021**, *60*, 20407–20416.

(110) Bojesen, E. D.; Iversen, B. B. The chemistry of nucleation. *CrystEngComm* **2016**, *18*, 8332–8353.

(111) Murphy, C. J.; Buriak, J. M. Best Practices for the Reporting of Colloidal Inorganic Nanomaterials. *Chemistry of Materials* **2015**, *27*, 4911–4913.

(112) Wang, F. D.; Tang, R.; Buhro, W. E. The Trouble with TOPO; Identification of Adventitious Impurities Beneficial to the Growth of Cadmium Selenide Quantum Dots, Rods, and Wires. *Nano Letters* **2008**, *8*, 3521–3524.

(113) Wang, F.; Tang, R.; Kao, J. L. F.; Dingman, S. D.; Buhro, W. E. Spectroscopic Identification of Tri-n-octylphosphine Oxide (TOPO) Impurities and Elucidation of Their Roles in Cadmium Selenide Quantum-Wire Growth. *Journal of the American Chemical Society* **2009**, *131*, 4983–4994.

(114) Baranov, D.; Lynch, M. J.; Curtis, A. C.; Carollo, A. R.; Douglass, C. R.; Mateo-Tejada, A. M.; Jonas, D. M. Purification of Oleylamine for Materials Synthesis and Spectroscopic Diagnostics for trans Isomers. *Chemistry of Materials* **2019**, *31*, 1223–1230.

(115) Lang, E. N.; Porter, A. G.; Ouyang, T.; Shi, A.; Hayes, T. R.; Davis, T. C.; Claridge, S. A. Oleylamine Impurities Regulate Temperature-Dependent Hierarchical As-

sembly of Ultranarrow Gold Nanowires on Biotemplated Interfaces. *ACS Nano* **2021**, *15*, 10275–10285.

(116) De Roo, J.; Ibáñez, M.; Geiregat, P.; Nedelcu, G.; Walravens, W.; Maes, J.; Martins, J. C.; Van Driessche, I.; Kovalenko, M. V.; Hens, Z. Highly Dynamic Ligand Binding and Light Absorption Coefficient of Cesium Lead Bromide Perovskite Nanocrystals. *Acs Nano* **2016**, *10*, 2071–2081.

(117) Drijvers, E.; De Roo, J.; Martins, J. C.; Infante, I.; Hens, Z. Ligand Displacement Exposes Binding Site Heterogeneity on CdSe Nanocrystal Surfaces. *Chemistry of Materials* **2018**, *30*, 1178–1186.

(118) Shen, Y.; Gee, M. Y.; Greytak, A. B. Purification technologies for colloidal nanocrystals. *Chemical Communications* **2017**, *53*, 827–841.

(119) Aubert, T.; Golovatenko, A. A.; Samoli, M.; Lermusiaux, L.; Zinn, T.; Abécassis, B.; Rodina, A. V.; Hens, Z. General Expression for the Size-Dependent Optical Properties of Quantum Dots. *Nano Letters* **2022**, *22*, 1778–1785.

(120) Maes, J.; Castro, N.; De Nolf, K.; Walravens, W.; Abecassis, B.; Hens, Z. Size and Concentration Determination of Colloidal Nanocrystals by Small-Angle X-ray Scattering. *Chemistry of Materials* **2018**, *30*, 3952–3962.

(121) Holder, C. F.; Schaak, R. E. Tutorial on Powder X-ray Diffraction for Characterizing Nanoscale Materials. *ACS Nano* **2019**, *13*, 7359–7365.

(122) Billinge, S. J. L.; Levin, I. The Problem with Determining Atomic Structure at the Nanoscale. *Science* **2007**, *316*, 561–565.

(123) Christiansen, T. L.; Cooper, S. R.; Jensen, K. M. . There's no place like real-space: elucidating size-dependent atomic structure of nanomaterials using pair distribution function analysis. *Nanoscale Advances* **2020**, *2*, 2234–2254.

(124) De Roo, J.; Yazdani, N.; Drijvers, E.; Lauria, A.; Maes, J.; Owen, J. S.; Van Driessche, I.; Niederberger, M.; Wood, V.; Martins, J. C.; Infante, I.; Hens, Z. Probing Solvent–Ligand Interactions in Colloidal Nanocrystals by the NMR Line Broadening. *Chemistry of Materials* **2018**, *30*, 5485–5492.

Graphical TOC Entry